

Why is the ~~Are city's~~ responsibility ~~le~~ for ~~their~~ ~~its~~ air pollution ~~often~~ underestimated? A focus on PM_{2.5}

Philippe Thunis¹, Alain Clappier², Alexander de Meij³, Enrico Pisoni¹, Bertrand Bessagnet¹, Leonor Tarrason⁴.

¹ European Commission, Joint Research Centre, Ispra, Italy

² Université de Strasbourg, Laboratoire Image Ville Environnement, Strasbourg, France

³ MetClim, Varese, Italy

⁴ NILU, Norway

Correspondence to: Philippe Thunis (philippe.thunis@ec.europa.eu)

Abstract

While the burden caused by air pollution in urban areas is well documented, the origin of this pollution and therefore the responsibility of the urban areas in generating this pollution is still a subject of scientific discussion. Source Apportionment represents a useful technique to quantify the city responsibility but the approaches and applications are not harmonized, therefore not comparable, resulting in confusing and sometimes contradicting interpretations. In this work, we analyze how different source apportionment approaches apply to the urban scale and how their building elements and parameters are defined and set. We discuss in particular the options available in terms of indicator, receptor, source and methodology. We show that different choices for these options lead to very large differences in terms of outcome. ~~In average over~~ ~~the~~ ~~For the~~ 150 EU large cities selected in our study, ~~the~~ ~~different~~ choices made for the indicator, the receptor and the source each lead to an average factor 2 difference in terms of city contribution. We also show that temporal and spatial averaging processes applied to the air quality indicator, especially when diverging source apportionments are aggregated into a single number lead to favor strategies that target background sources while occulting actions that would be efficient at the city center. We stress that methodological choices and assumptions most often lead to a systematic and important underestimation of the city responsibility, with important implications. Indeed, if cities are seen as a minor actor, plans will target in priority the background at the expense of potentially effective local actions.

Keywords: air pollution, source apportionment, particulate matter

1. Introduction

About 55% of the world's population lives in urban areas nowadays, and this number is expected to increase to 68% by 2050, according to the United Nations (UN 2018). Large population growth is also projected by 2030 in most of the major European cities (Alberti et al., 2019) with predicted population growth varying in range from Berlin (15%), Paris (19%), Milan/Rome

Formatted: Subscript

Formatted: English (United Kingdom)

41 (21%), Prague (37%), London (39%), to Brussels (52%) (see
42 <https://urban.jrc.ec.europa.eu/thefutureofcities/urbanisation#the-chapter>). As a result of this
43 population trend, urban emissions and their associated pollution levels are expected to increase
44 as well.

45
46 According to a recent estimate (EEA, 2020), about 74 % of the EU-28 urban population are
47 exposed to pollution of fine particulate matter (PM_{2.5}) in concentrations above the WHO Air
48 Quality Guidelines value, this number raises to 99% for ozone (O₃) and is about 4% for nitrogen
49 dioxide (NO₂). Air pollution is a heavy burden on human health with more than 380,000
50 premature deaths in EU-28 reported in 2017 according to the same EEA estimates. For a wide
51 range of European cities, Khomenko et al. (2021) showed that the health burden due to air
52 pollution varies greatly by city, with annual premature mortality reaching up to 15% for PM_{2.5}
53 and 7% for NO₂. The highest mortality burden for PM_{2.5} occurs in northern Italy, southern
54 Poland and eastern Czech Republic. De Bruyn and de Vries (2020) showed that for all 432 cities
55 in their sample (total population: 130 million inhabitants), the social costs (e.g. hospital
56 admissions, premature mortality) but also due to air pollution exceeded € 166 billion in 2018 for
57 Europe (EU27 plus the UK, Norway and Switzerland). City size was shown to be a key factor
58 contributing to the total social costs: all cities with a population over 1 million features in the
59 Top 25 cities with the highest social costs due to air pollution.

60
61 Given the health and economic burden caused by air pollution in urban areas, it is important to
62 identify the origin of this pollution in order to reduce and control its impact. Identifying the
63 sources of urban pollution and then assigning responsibilities enables a process to implement
64 measures and control air pollution. Assessing the responsibility or share of cities for their
65 pollution has important implications. For being effective, pollution reduction plans must be
66 designed and applied to target the most polluting sectors at the relevant spatial (national, regional
67 and/or local) and with the appropriate temporal scales. In this context, quantifying the share of
68 the city pollutions caused by their own emissions becomes a crucial element to determine
69 whether actions need to be applied locally or at the regional, national country or continental
70 scales. This has important governance consequences for the effective control of air pollution.

71
72 For pollutants like NO₂, that mostly originate from traffic sources and have a relatively short
73 lifetime in the atmosphere, there is a general agreement on the fact that cities are the main
74 contributor to this pollutant concentration levels and that acting locally on traffic emissions is the
75 most efficient way of improving NO₂ concentration levels in a particular city (Tobias et al.,
76 2020). There is available European-wide information such as in Degraeuwe et al. (2019)
77 providing overviews of the potential impact of traffic emission reductions per vehicle type in
78 different European cities. There is also agreement regarding O₃ that this secondary pollutant is
79 most effectively reduced by implementing reduction measures at larger spatial scales, involving
80 actions driven at the regional and even continental scales (e.g. Luo et al. 2020). For other
81 pollutants, like PM_{2.5}, complex physical and chemical atmospheric processes with different time
82 scales drive its formation, involving numerous precursors themselves emitted by several sources.
83 The sources of PM_{2.5} pollution range from local traffic, domestic fuel burning and industrial
84 activities to regional sources such as agriculture in rural areas. Even though the latter emissions
85 do not originate from cities, Thunis et al. (2018) showed that their impact on urban pollution
86 could be important, reaching up to 30% in several European cities. Because of this complexity,

87 there is less consensus regarding the responsibility or share of a city to its pollution when
88 addressing PM_{2.5}. Because of this lack of consensus and the major burden of PM_{2.5} on health, we
89 focus our analysis on this pollutant.

90
91 The usual approach to assess the city share to its pollution levels (in other words the city
92 responsibility) is source apportionment (SA). However, many SA approaches exist. The most
93 widely used SA methods are the “potential impact” (or brute force), the “increment” and
94 “tagging” approaches. An overview description of these methods and an evaluation of their
95 limitations and capabilities for use can be found in Thunis et al. (2019). ~~and n~~ Moreover, many
96 ways to parameterize them exist as well, leading to a variety of results and interpretations. ~~The~~
97 ~~most widely used SA methods are the “potential impact” (or brute force), the “increment” and~~
98 ~~“tagging” approaches. An overview description of these methods and an evaluation of their~~
99 ~~limitations and capabilities for use can be found in Thunis et al. (2019).~~ For the 18 million
100 inhabitant’s city of New Delhi, Amann et al. (2017) concluded that only 40% of the PM_{2.5}
101 pollution was originating from local city sources, based on potential impacts SA and expressed
102 in terms of city averaged population exposure, averaged yearly. In the context of the Copernicus
103 programme, CAMS (Copernicus Atmosphere Monitoring Service) performs SA calculations
104 daily with two different approaches, namely tagging and potential impacts, for a series of
105 European cities. Results show important differences on a day-by-day basis although these
106 differences smooth out when considering longer term averages (Pommier et al. 2020). Based on
107 the increment approach, Kiesewetter and Amann (2014) derived SA estimates for a series of
108 European cities and aggregated these detailed results at country levels, leading to relatively low
109 city responsibilities (e.g. about 25% for French, German or Italian cities). Based on a potential
110 impact approach, Thunis et al. (2018) estimated city shares for 150 cities in Europe. They
111 highlighted their large variability across Europe and stressed the importance of the definition of
112 the city on the results, by testing the sensitivity to different city extensions. The choice of the SA
113 method but also the way this method is configured, can lead to very different outcomes for the
114 city share to its pollution, ranging from cities being a major contributor to their pollution to cities
115 having a limited responsibility. This explains why the actual city responsibility on its pollution is
116 yet discussed, and why some authors stress the importance of local actions (Thunis et al., 2018,
117 Wu et al. 2011, Raifman et al., 2020) when others stress the need for regional, national or even
118 continental actions (Huszar et al. 2016, ApSimon et al. 2021, Liu et al., 2013). This diversity of
119 conclusions has serious consequences in terms of policy decisions. Blaming external (i.e. outside
120 the city) pollution sources as main responsible for urban pollution is sometimes an easy
121 argumentation for decision-makers to justify local inaction.

122
123 This work aims at explaining the main causes of discrepancies between different assessments of
124 the city emission’s impact on its pollution levels and show that these discrepancies generally lead
125 to underestimating the city’s responsibility. It proposes a specific harmonized nomenclature for
126 source ~~allocation~~ apportionment approaches, and it shows how it is important to document the
127 choices to enable correct interpretation of the results. We begin with a conceptual overview of
128 the parameters structuring any SA approach (Section 2). This includes the definition of the key
129 parameters to any SA study: indicator, source, receptor, and methodology to relate them. Then
130 (Section 3) we assess the sensitivity of the urban SA results to the choices of these four
131 parameters. In Section 4, we analyze implications in terms of air quality planning and suggested
132 strategies. We finally provide conclusions in Section 5.

133 2. Assessing the city responsibility on air pollution: Main concepts

134 In this section, we detail the steps required to quantify the responsibility of a city on its air
135 pollution, through source apportionment (SA). SA is a methodology that serves to estimate the
136 contribution of a given source at a specific receptor for a given indicator (for example the
137 concentration of a given pollutant like PM or NO₂). It involves the following steps (Figure
138 1):

- 139 (1) defining a relevant indicator, denoted as (I) to characterize air pollution
- 140 (2) defining the receptor (R) through its spatio-temporal characteristics, i.e. the area (\bar{x}_r)
141 and time period (\bar{t}_r) over which the indicator is averaged
- 142 (3) defining the source (S), ~~in our case the city, through and~~ its spatio-temporal
143 characteristics, i.e. the city area (x_s) and time period for which the city responsibility
144 is assessed (t_s)
- 145 (4) selecting the source apportionment (SA) methodology to capture the processes that
146 relate the source to the receptor.
147

148 Figure 1 summarizes these steps, as well as the nomenclature and symbols used in this
149 work. We use this new nomenclature to attach contextual information (i.e. metadata) to the
150 source apportionment. Further explanations of the symbols are given in the subsections below.
151

Formatted: Font: (Default) Times New Roman, 12 pt,
Not Italic, Font color: Auto, English (United States)

Formatted: Font: (Default) Times New Roman, 12 pt,
Not Italic, Font color: Auto, English (United States)

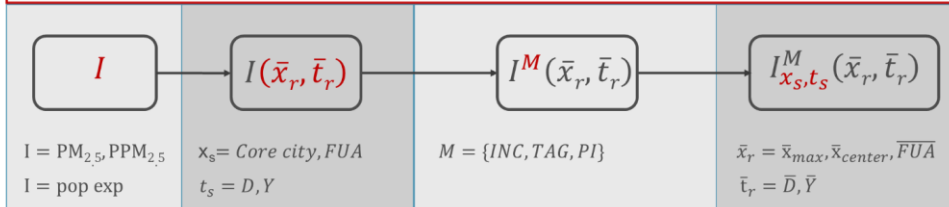
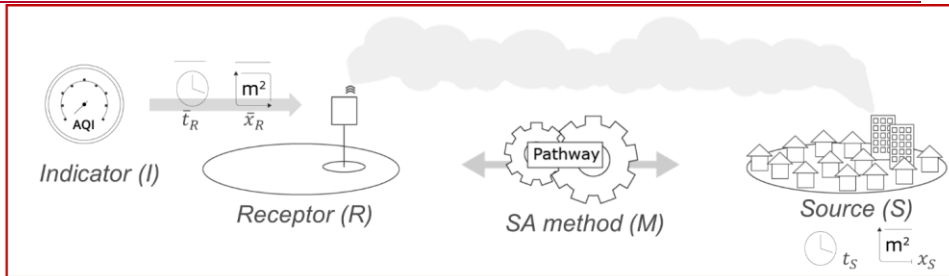
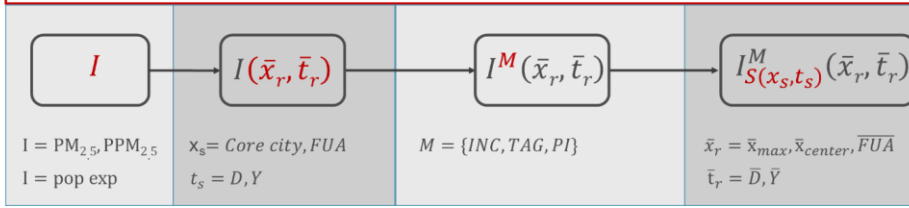
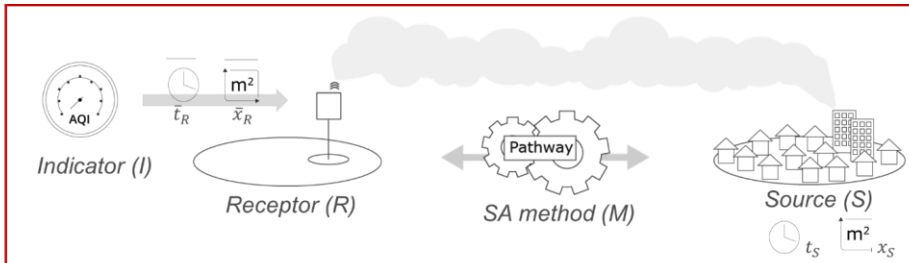


Figure 1: Schematic flow chart representing the four steps required to fully define any SA process. The red letters indicate the indicator characteristic under consideration. The general notation for the indicator (I) includes a superscript for the methodological approach (M), a subscript to inform on the source (S) and brackets to inform on the receptor (R). The spatial and temporal dimensions associated to the source and receptor are denoted by "x" and "t", respectively. The overbar indicates an averaging process. The lowest row provides for each parameter examples used in this work. *Some images used in this schematic flow chart are adapted from flaticon.com.*

2.1 Definition of the air pollution indicator (I)

The first step required to assess the role/responsibility of city emissions with respect to its air pollution, is to define an indicator that identifies the pollution aspect we are interested in. The indicator can be defined in many ways. For example, as the total concentration of a given compound (e.g. PM), or as a specific constituent of that total concentration (e.g. PM_{2.5} or its primary fraction, PPM), or as a composite based on a mix of different pollutants (e.g. maximum

166 among O₃, PM_{2.5} and NO₂ concentrations as in some air quality indexes such as ATMO2003) or
167 as population exposure (i.e. product of population and concentration).

168 2.2 Definition of the receptor (R)

169 Estimating the indicator, either from a measuring instrument or from a model simulation, implies
170 an averaging process, both in space and time. For model data, averages correspond to the spatial
171 and temporal resolutions (e.g. the time step and grid cell size) whereas for measurement, the
172 space-time average will depend on the instrument acquisition time and on the atmospheric
173 dispersion characteristics at the measuring site. Regardless of these intrinsic time and space
174 averages, indicators are generally averaged over longer spatial and temporal scales for
175 convenience. The receptor is defined as the spatio-temporal entity over which the indicator is
176 averaged. Both a spatial and a temporal scale (denoted by \bar{x}_r and \bar{t}_r , respectively) must be
177 associated to the receptor to define it.

178
179 For the temporal dimension, typical examples for PM_{2.5} are days ($\bar{t}_r = \bar{D}$) or years ($\bar{t}_r = \bar{Y}$).
180 Spatially, the indicator can be estimated at a specific location, e.g. the city center ($\bar{x}_r = \bar{x}_{center}$),
181 at the location where the maximum concentration occurs ($\bar{x}_r = \bar{x}_{max}$) or averaged over the city
182 ($\bar{x}_r = \overline{city}$). For convenience, we use indifferently the following notations to refer to the
183 receptor:

$$184 \quad R(\bar{x}_r, \bar{t}_r) = R = \bar{x}_r, \bar{t}_r \quad (1)$$

185 2.3 Definition of the source (S)

186 The source is defined as the spatio-temporal entity (e.g. city, emission macro-sector...) for which
187 we assess the contribution to the indicator. For the purpose of this work, the source is defined as
188 the city, and more precisely as the emissions that originate from a given city. The source
189 emissions (denoted by E) are indeed responsible for the pollution fraction that can be associated
190 to the source/city at the receptor (R). These emissions are characterized by a spatial ($x_s =$
191 extension of the city) and a temporal scale ($t_s =$ period of time over which the source activity is
192 assessed). For convenience, we use indifferently the following notations to refer to the source:

$$193 \quad S(x_s, t_s) = S = E = city = x_s, t_s \quad (2)$$

194
195 In this work, we analyse in particular the impact of the city extension (x_s) on the apportionment
196 outcome. For this purpose, we define cities in two ways:

- 197
198 (1) as core cities, i.e. the local administrative units, with a population density above
199 1500/km² and a population above 50,000, where the majority of the population lives in an
200 urban center and
201 (2) as functional urban areas (OECD, 2012, denoted as “FUA”) composed as core cities plus
202 their wider commuting zone, consisting of the surrounding travel-to-work areas where at
203 least 15% of the employed residents work in the city.

204 Details on the FUA and core city areas are available for 150 EU cities in the urban PM_{2.5} atlas
 205 (Thunis et al. 2017). Note that other city definitions exist. In the context of the CAMS source
 206 allocation analysis, city are defined as an arbitrary number of grid cells in the modelling domain
 207 (Pommier et al., 2020).

208 Finally, we define the city background as the sum of all contributions from sources that are not
 209 covered by the spatial (x_s) and temporal (t_s) scales of the city source.

210
 211 One main difference between sources and receptors is that for the latter, spatio-temporal
 212 characteristics are averaged. Apart from this, temporal and spatial characteristics can also differ
 213 in terms of value. For example, the source can be defined as the FUA ($x_s = \text{FUA}$) while the
 214 receptor is a specific location ($\bar{x}_r = \bar{x}_{max}$). Temporally, interest can be on assessing the
 215 contribution of the city weekly activity ($t_s = 1$ week) for a given day ($\bar{t}_r = \bar{D}$) at the receptor. In
 216 the results presented here, the source and receptor temporal scales are however chosen identical
 217 for convenience.

218 2.4 Selection of the SA methodology

219 When the air pollution indicator and the spatio-temporal characteristics of both the receptor and
 220 the source have been selected, the next step consists in distinguishing and quantifying the
 221 fractions of the indicator related to the city source ($I_{city}(R)$) and to the background ($I_{bg}(R)$) at
 222 receptor R, respectively. This decomposition is summarized by the following equation:
 223

$$I(R) \rightarrow \{I_{city}(R), I_{bg}(R)\} \quad (3)$$

224
 225 Different SA methodologies exist to perform this operation. In this section, we describe three
 226 main approaches but only in brief, as details about each of these are discussed in other works
 227 (Clappier et al. 2017; Thunis et al., 2019, 2018; Mertens et al. 2018). As mentioned previously,
 228 we use the indicator's superscript to refer to its calculation method [$I_{city}^M(R)$]. Methods are
 229 summarized in Table 1.

230
 231 **Potential impacts (PI):** The city contribution in this method is denoted as $I_{city}^{PI100}(R)$ and is
 232 calculated as the difference between two simulations: a base-case that includes the city
 233 [$I(R)$] and a scenario in which the city emissions are switched off [$I_{city^{100}}(R)$]. In this notation,
 234 the source superscript (here, 100) indicates the percentage intensity by which the source
 235 emissions are reduced. Reductions are intended as percentage variations from the base-case
 236 situation. The same approach can be used with reduction percentages that are lower than 100%.
 237 In this case the resulting difference is divided by the reduction percentage to obtain the potential
 238 impact ($I_{city}^{PI\alpha}(R)$). A similar approach is used to calculate the background contribution, i.e. by
 239 removing or reducing partially the background emission sources. Potential impacts methods for
 240 source apportionment are widely used (Osada et al. 2009; Huszar et al. 2016, Huang et al. 2018;
 241 Wang et al. 2014; Wang et al. 2015; Van Dingenen et al. 2018; Thunis et al. 2016; Clappier et al.
 242 2015; Pisoni et al. 2017).

243
 244 **Increment (INC):** With this methodology, the background contribution is estimated as the
 245 concentration observed/modelled at a given location "y" [$I_{bg}^{INC}(R) = I(\bar{y}, \bar{t}_r)$]. This location must
 246 be far enough from the source, not to feel its influence but be close enough to the source to avoid

247 influences from other sources, external to the city. These assumptions are further described and
 248 discussed in Thunis et al. (2017). The city contribution is then obtained as the difference between
 249 the base case indicator and the background contribution [$I_{city}^{INC}(R) = I(\bar{x}_r, \bar{t}_r) - I(\bar{y}, \bar{t}_r)$]. The
 250 increment methodology has been used e.g. by Lenschow et al. (2001), Petetin et al. (2014),
 251 Kieseewetter et al. (2015), Squizzato et al. 2015, Timmermans et al. 2013, Keuken et al. 2013,
 252 Ortiz and Friedrich 2013 and Pey et al. 2010.

253
 254 **Tagging (TAG):** With this approach, species emitted by the city are numerically tagged and
 255 followed through the modelled transport, dispersion and chemical transformation processes.
 256 When chemical transformations take place, preserved atoms are used as tracers. For example, the
 257 nitrogen atom (N) will be used to follow the NO source emissions through its successive
 258 transformations into NO₂ and HNO₃ to reach its final product NO₃, that will then be attributed to
 259 that source. Example of tagging applications are e.g. Kranenburg et al. 2013, Yarwood et al.
 260 2004; Wagstrom et al., 2008; Kwok et al. 2013; Bhave et al. 2007; Wang et al., 2009. Some of
 261 these approaches are implemented operationally to estimate daily city contributions on air
 262 pollution (<https://topas.tno.nl/documentation/>).

263
 264 The formulations corresponding to these three main approaches are summarized in Table 1.

265
 266 A few key points are worth noting. While tagging and potential impacts approaches explicitly
 267 consider city emissions in their calculations, this is not the case for increments that only refer to
 268 them implicitly. By construction, both the increment and tagging approaches are additive [i.e.
 269 $I(R) = I_{city}(R) + I_{bg}(R)$] whereas this is not the case for potential impacts when pollutants
 270 behave non-linearly because of air transport, deposition or chemical processes (Clappier et al.,
 271 2017).

272
 273

	City contribution	Background contribution
Potential Impact	$I_{city}^{PI\alpha} = \frac{I(R) - I_{city}^{\alpha}(R)}{\alpha}$	$I_{bg}^{PI\alpha} = \frac{I(R) - I_{bg}^{\alpha}(R)}{\alpha}$
Increment	$I_{city}^{INC} = I(\bar{x}_r, \bar{t}_r) - I(\bar{y}, \bar{t}_r)$	$I_{bg}^{INC} = I(\bar{y}, \bar{t}_r)$
Tagging	$I_{city}^{TAG} = \sum_E^{city} I_E(R)$	$I_{bg}^{TAG} = \sum_E^{bg} I_E(R)$

274 *Table 1: Formulation of the three main methods to estimate the contribution/impact/increment of a city. The letters, I, S and R*
 275 *refer to the indicator, source and receptor, respectively. The indicator superscript refers to the SA method (PI for potential*
 276 *impacts, INC for increments and TAG for tagging) while its subscript indicates the source (city or background (bg)). α represents*
 277 *the percentage reduction factor applied for the source emissions in the potential impacts method. See text for additional details.*

278 3. Results

279 Recognizing the impossibility of assessing the sensitivity of the results for all combinations of
280 indicators, source, receptor and methodology, we focus our analysis on comparisons in which
281 only one parameter is changed at a time, to highlight major sensitivities. For this purpose, we use
282 the following two main sources of data and results.

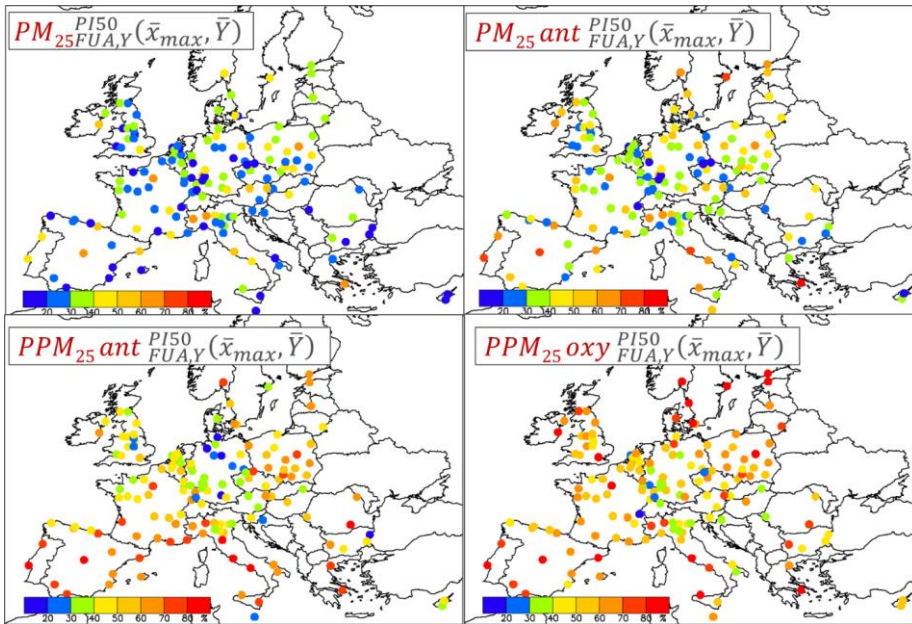
- 283
284 • **SHERPA:** SHERPA is a modelling tool, based on Source-Receptor Relationships that
285 represent a simplified version of a Chemistry Transport Model, used to simulate the
286 contribution to PM_{2.5} concentration levels by all precursor emissions (NO_x, NMVOC,
287 PPM, SO₂ and NH₃) from different cities in Europe (Clappier et al. 2015, Thunis et al.
288 2016, 2018). In its current configuration, SHERPA is based on the CHIMERE model
289 (Menut et al. 2013) covering the whole of Europe at roughly 7 km spatial resolution. In
290 this work, we use the source apportionment results over 150 cities as reported in the
291 PM_{2.5} urban atlas (Thunis et al., 2017) as well as additional SHERPA data to provide
292 further analysis.
- 293
294 • **EMEP simulations:** The EMEP model is an off-line regional transport chemistry model
295 (Simpson et al., 2012; <https://github.com/metno/emep-ctm>). The model has 20 vertical
296 levels, with the first level around 50 m. The model uses meteorological initial conditions
297 and lateral boundary conditions from the European Centre for Medium Range Weather
298 Forecasting (ECMWF-IFS). The meteorological year is 2015. Detailed information on
299 the meteorological driver, land cover, model physics and chemistry are described in
300 Simpson et al. (2012) and in the EMEP Status Report 2017
301 (https://emep.int/publ/reports/2017/EMEP_Status_Report_1_2017.pdf). In this work, we
302 use specific simulations where emissions have been removed partially or fully in a series
303 of European cities. Additional details regarding these simulations are provided together
304 with the discussion of the results.

305 Based on these sources of information and data, we discuss hereafter the sensitivity of the SA
306 results to the choice of the indicator (Section 3.1), to the choice of the methodology (Section
307 3.2), to the source (Section 3.3) and finally to the receptor (Section 3.4).

308 3.1 Sensitivity to the indicator

309 The implications resulting from the choice of the indicator are illustrated in Figure 2 for four
310 indicators, based on SHERPA results for 150 cities in Europe. The four indicators selected to
311 characterize air pollution are: a) the PM_{2.5} concentration (top left, from Thunis et al. 2017), b) the
312 anthropogenic fraction of PM_{2.5} (“PM_{2.5} ant”, top right), c) the primary anthropogenic fraction of
313 PM_{2.5} (“PPM_{2.5} ant” bottom left) and d) the primary fraction of PM_{2.5} originating from the
314 transport and residential sectors (“PPM_{2.5} oxy”, bottom left). The reference (PM_{2.5} total mass, top
315 left) corresponds to the indicator currently used in legislation (e.g. European Ambient Air
316 Quality Directive, AAQD2008) against which health impacts are correlated (WHO2005). In the
317 second case, the indicator is limited to its anthropogenic fraction (PM_{2.5} ant), excluding therefore
318 natural contributions (dust, marine salt...). This is motivated by the fact that policies have no
319 impact on this component. According to this indicator, city contributions increase significantly

320 (by about 20% in average) and in some cities where natural dust pollution is important (e.g. in
 321 Sicily), the city responsibility shifts from minor to major. If we further restrict the indicator to its
 322 primary anthropogenic fraction (“PPM_{2.5 ant}”, bottom right) because of its suggested higher
 323 health burden (Park et al., 2018; Viana et al., 2008), the city contribution then increases
 324 significantly in most cities. This becomes even more striking if we limit the indicator to the
 325 PPM_{2.5} fraction originating from the transport and residential sectors (bottom right). These two
 326 sectors have recently been shown to generate the largest burden on human health given the high-
 327 oxidative potential of their emissions (Rankjar et al., 2020, Li et al. 2016). With this indicator,
 328 the majority of EU cities become main contributors to their pollution. Regarding the latter
 329 indicator, it is important to note that although the increasing adoption of electric vehicles shows
 330 rather positive impacts on health (Choma, 2020), the remaining PM emissions from road traffic
 331 like tires and brake and road wear emissions (Kole et al., 2017; EC, 2014; Ntziachristos and
 332 Boulter, 2019) will remain an issue. The calculation of various geochemical indices (enrichment
 333 factor, geo-accumulation index, pollution index and potential ecological risk) also show that road
 334 dust is extremely enriched and contaminated by elements from tire and brake wear (e.g. Sb, Sn,
 335 Cu, Bi and Zn).
 336



337
 338 Figure 2: SHERPA results for 150 major cities in Europe for the overall PM_{2.5} concentration (top left), for its anthropogenic
 339 fraction (“PM_{2.5 ant}”, top right), for its anthropogenic primary fraction (“PPM_{2.5 ant}”, bottom right) and for its primary
 340 fraction originating from the transport and residential sectors (“PPM_{2.5 oxy}”, bottom left). For all cities, the source is defined
 341 spatially as the FUA over which emissions are reduced over a year (Y). The receptor is defined as the city location where the
 342 concentration is maximum (\bar{x}_{max}) and the indicator is averaged yearly at the receptor (\bar{Y}). All calculations are made with the
 343 same SA methodology, namely, potential impacts (PI) with city emissions reduced by 50% (PI50)

344 3.2 Sensitivity to the SA methodology

345 A comparison of SA methodologies is proposed in Thunis et al. (2019) where the potential
346 impact, increment and tagging approaches are compared both on simple theoretical examples and
347 on real data to highlight differences among methods and stress their limitations. In this section,
348 we summarize the main findings of this work and complement it with comparisons that focus on
349 the apportionment of the city vs. background contributions. We also provide in the appendix a
350 comparison of all SA methods discussed in this section, applied on a theoretical example tuned
351 to the city scale.

352 Increment vs. potential impacts

353 Thunis (2017) compared increments and potential impacts with the SHERPA model for a series
354 of European cities. ~~They-He~~ showed that increment approaches lead to important
355 underestimations (30 to 50%) of the city responsibility for PM_{2.5} and NO₂ with respect to
356 potential impacts. This underestimation is explained by the non-fulfilment of the two underlying
357 increment assumptions, related to the external location [i.e. y in $I_{bg}^{INC}(R) = I(\bar{y}, \bar{r}_r)$] that must: 1)
358 be far enough from the city, not to feel its influence but 2) close enough to the city to avoid
359 influences from sources external to the city. The Authors show that these two assumptions are
360 seldom fulfilled in reality.

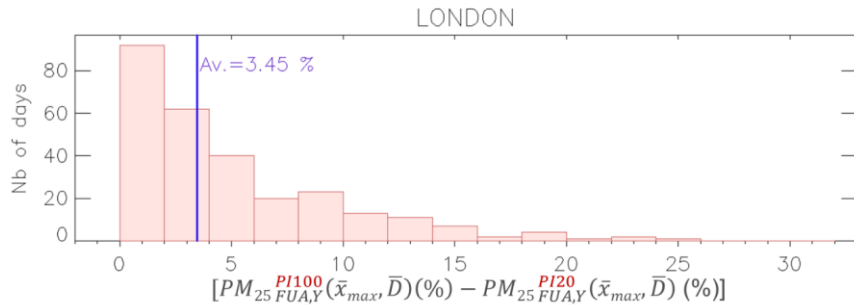
361 Tagging vs. potential impacts

362 Clappier et al. (2017) discussed the concepts underlying these two SA methods and showed that
363 important differences in terms of results arise as soon as non-linear processes are present. Belis
364 et al. (2020) highlighted and quantified these large differences based on a real-case inter-
365 comparison exercise. Finally, Thunis et al. (2019) reviewed in their work many inter-
366 comparisons between tagging and potential impact SA results. In their application over the Po
367 basin (Italy), they showed that differences are large for the agriculture sector (dominated by NH₃
368 emissions) but are also important for other sectors, when dealing with high temporal resolution
369 (e.g. daily) at the receptor. Unfortunately, these examples did not address the particular case of a
370 city scale apportionment.

371 Full vs. partial potential impacts

372 To analyze differences between full and partial impacts, we use a series of EMEP simulations in
373 which we remove totally (PI100) or partly (PI20) the London FUA emissions (source) during an
374 entire year. Figure 3 shows the differences between city contributions obtained with the two PI
375 methods. Differences can be important (up to 25 percentage points for specific days). Although
376 the number of high-difference days is limited (leading to a yearly average difference of few
377 percents), these days might represent high pollution episodes for which assessing the city
378 responsibility is important to act. In general, the higher resolution applied to the temporal and/or
379 spatial averages at the receptor, the largest the differences are among methods. It is also
380 interesting to note that partial potential impacts systematically underestimate full potentials (no
381 negative values).

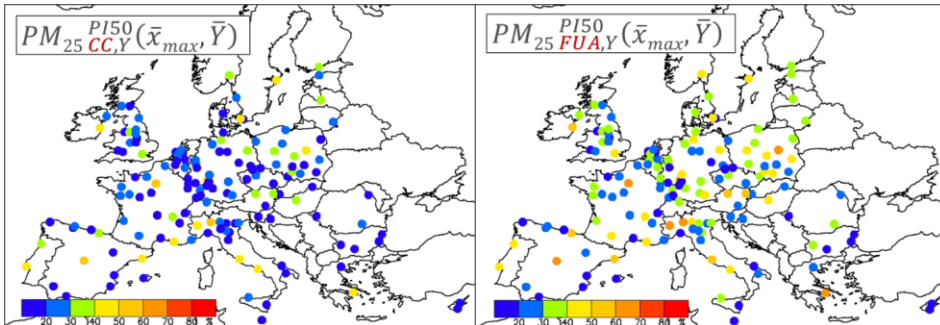
382



389
390
391
392
393
394
Figure 3: Histogram of daily city contribution differences to London $PM_{2.5}$ levels between two potential impacts methods, PI100 and PI20, calculated with the EMEP model. The source is defined spatially as the FUA where emissions are reduced yearly (Y subscript). The receptor is defined as the city location where the maximum yearly averaged concentration is modelled (\bar{x}_{max}), and temporally as daily average (\bar{D}). Each column represents the number of days with a specific PI difference (PI100 - PI20). The blue line provides the yearly average difference.

395 3.3 Sensitivity to the source

396 Figure 4 shows the comparison between SA obtained with sources defined as core cities (left)
397 and as FUA (right). The city contribution / responsibility is multiplied by a factor 2 on average
398 (see also Figure 8) when FUA are considered. The larger spatial extension of the FUA and its
399 implied additional emissions explain the differences that lead some cities to become a major
400 actor, i.e. where the city contribution dominates the background one (e.g. Athens, Warsaw,
401 Milan, Turin and Rome).
402



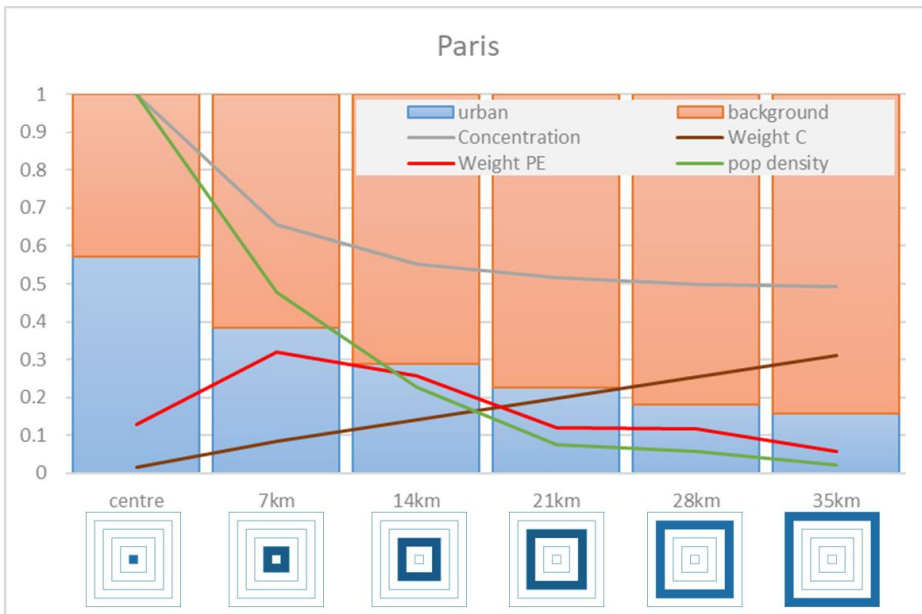
403
404
405
406
407
408
Figure 4: Maps of city contributions obtained for spatial sources defined in 2 ways: core city (CC, left) and FUA (right). Results are shown for 150 cities in Europe, based on the SHERPA-CHIMERE model using a potential impact SA method for a reduction strength of 50% (PI50). The indicator is the total $PM_{2.5}$ concentration. The receptor is selected as the location where the maximum yearly average concentration occurs (\bar{x}_{max}) and applies yearly time average (\bar{Y}). The source emissions are reduced over a full year (Y).

409 3.4 Sensitivity to the receptor

410 In this section, we discuss the spatial and temporal averages applied at the receptor. Spatially,
411 different averaging options exist, ranging from a single location (i.e. one modeling grid cell) to
412 more or less extended areas covering part of the source or even larger. To illustrate the

413 sensitivity of SA to that choice, we use the case of Paris (Figure 5) where emission have been
 414 reduced over the FUA (source) over a full year.

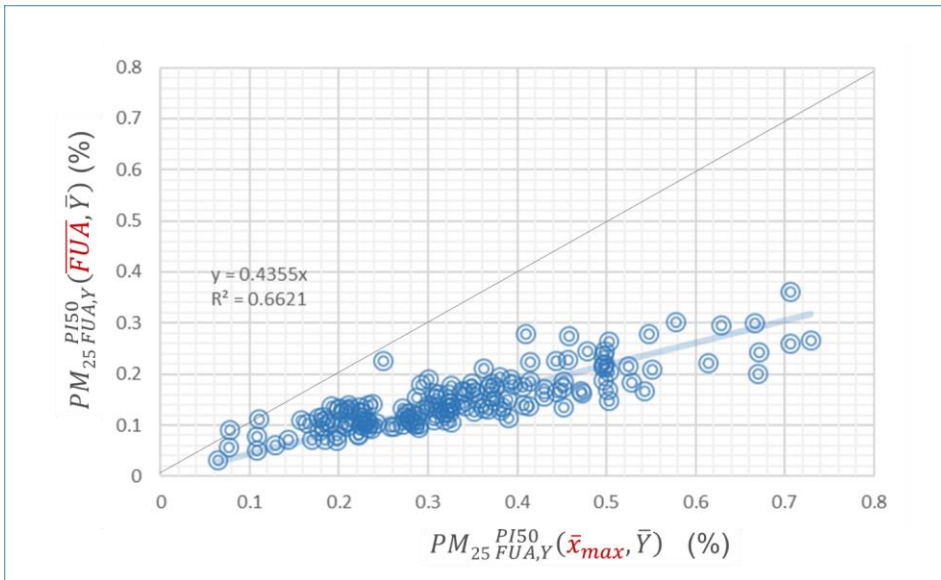
415
 416 SA varies largely from one location to another within Paris. We highlight this with bars that
 417 distinguish the city vs. background contributions for locations at different distance from the city
 418 centre. We note opposite trends, dominated by the city source (around 60%) at the city center
 419 and dominated by the background source towards the periphery (around 80%). While the SA at
 420 the city centre is representative of a single cell within the city, this is not the case for SA close to
 421 the periphery. This is highlighted by the city rings (below the X-axis) that indicate the area of
 422 representativeness of a given SA. When we average spatially an indicator (PM_{2.5} or population
 423 exposure) over a receptor that covers the entire FUA (all 6 rings), these areas of
 424 representativeness enter into play. The brown curve indicates the weight (in the spatial average)
 425 attached to each city ring, relatively to the city total (i.e. all rings). Weights increase fast when
 426 moving towards the periphery because of the larger ring areas. The spatial averaging process
 427 leads to over-representing the periphery, which overweight the city center SA by almost a factor
 428 40. It is interesting and counter-intuitive to note that with this averaging process, the city
 429 responsibility decreases when the city area increases. With population exposure as indicator
 430 (weights shown by red curve), the rapid population density decrease balances the ring area
 431 increase when moving outward, leading to weights that dominate for middle rings. ~~It is~~
 432 interesting to note, that w
 433 With average population exposure, the city center weight is yet similar
 434 to the weight obtained 28 km away.



435
 436 Figure 5: City rings' source apportionment for Paris PM_{2.5} and associated population exposure. The city/background
 437 apportionment (bars) is represented for rings (i) progressively more distant from the city centre (X axis). The ring average
 438 concentration (C_i) and population density (P_i) relative to the city centre values are represented in blue and green, respectively.

439 The relative (to the FUA total, i.e. all rings) weight of each ring (i) in the city average concentration (brown) is calculated as
 440 $C_i * S_i / \sum_i (C_i * S_i)$ where S_i is the ring area, respectively. A similar expression: $C_i * S_i * P_i / \sum_i (C_i * S_i * P_i)$ is used to determine
 441 the weight of each ring in the calculation of the average population exposure (red curve).

442 Figure 6 compares SA for 150 cities obtained for receptors defined (1) as the location where the
 443 maximum concentration is reached within the FUA (\bar{x}_{max}) and (2) as the FUA spatial average
 444 (\bar{FUA}). In average, city impacts for a spatially averaged receptor are about 55% lower.
 445 Depending on the spatial characteristic of the receptor, some cities will be considered as minor or
 446 major actors with respect to their pollution. We discuss this [issue point](#) further in Section 4.
 447



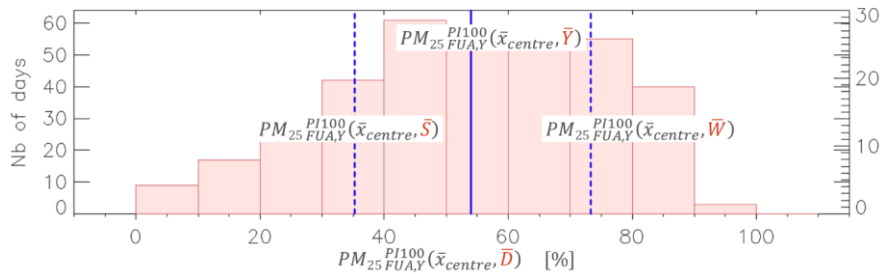
448
 449 Figure 6: Comparison of potential impacts for 150 cities in Europe obtained for a receptor spatially defined as the location where
 450 the concentration is maximum in the city (\bar{x}_{max} – X axis) and defined as the FUA spatial averaged (\bar{FUA}). For these calculations,
 451 the source are defined as the FUA over which emissions are switched off during the whole year. The indicator is the total $PM_{2.5}$
 452 mass. All results are based on the SHERPA-CHIMERE model using a potential impact SA method for a reduction strength of 50%
 453 (PI50) and are based on yearly averages at the receptor (\bar{Y}).

454 As seen from these results, spatial averages at the receptor significantly reduce the city
 455 responsibility, potentially leading to underestimating the city ability to reduce pollution levels
 456 via local controls. The large differences resulting from the choice of the receptor settings prevent
 457 meaningful comparisons. It is for example challenging to compare CAMS city contributions that
 458 are averaged spatially over the city area with the urban results obtained in the context of the
 459 Thematic Strategy on Air Pollution (Kiesewetter and Amann 2014) that are aggregated at
 460 country level or with SHERPA estimates based on a single grid cell receptor. It is therefore
 461 crucial to associate all SA settings (metadata) to the results in order to inform on the
 462 meaningfulness of a comparison. We discuss further this issue in the context of air quality
 463 planning in Section 4.
 464

465 Similar considerations apply to temporal averages. Figure 7 compares SA obtained when the
 466 indicator at the receptor is averaged yearly and seasonally with daily single values. For a yearly
 467 average, Madrid city's contribution is 54% but the spectra of daily contributions show variations
 468 that range from 10 to beyond 90%. Even seasonal averages show important differences with a
 469 factor 2 between summer and winter. Similarly, to spatial averages, temporal averages
 470 encompass a large spectra of SA outcome. Indicators averaged yearly at the receptor have been
 471 used for example in SHERPA (Thunis et al. 2017), GAINS (Kieseewetter and Amann, 2014)
 472 whereas daily indicators are used in CAMS (Pommier et al., 2020). Correlating low and high
 473 city contributions to meteorological factors (cold vs warm days, windy vs calm situations...) is
 474 beyond the scope of this work. This point is however addressed in Pisoni et al. (2021).

475
 476 Note that spatial averages have a larger smoothing effect than temporal ones because they are
 477 bidimensional.

478



479
 480 Figure 7: Frequency histogram of daily potential impact at 100% (PI100) modelled with the EMEP model for the city of Madrid.
 481 Each column represents the number of days with a given daily PI. The blue line provides the yearly average PI. For these
 482 calculations, the source is the Madrid Functional Urban Area (FUA) over which emissions are switched off during the whole year
 483 (Y). The indicator is the total $PM_{2.5}$ mass. The receptor point is the city centre location (\bar{x}_{centre}).

484

485 3.5 Methodological Assumptions and uncertainties

486 In addition to referring to the SA method itself (Section 2.4), other modelling parameters need to
 487 be documented as well. We list hereafter the main ones.

488

489 Most SA methods rely on models and are therefore characterized by a set of common strengths
 490 and weaknesses. One of the main limitations-assumption attached to models is the spatial
 491 resolution and its potential impact on the calculation of the city contribution. While a coarse
 492 resolution might be able to capture relatively well the background (characterized by smoother
 493 fields), this will not be the case for peak concentrations within the city. The coarser the model
 494 spatial resolution, the largest the underestimation of the city responsibility will be (De Meij et al.,
 495 2007).

496

497 Uncertainties may also result from our incomplete knowledge of some model input parameters,
 498 in particular chemical processes and emission sources. Some urban emission sources are not well
 499 documented and are probably underestimated. This is the case of residential emissions for which
 500 the inclusion of condensable remains a question mark (Bessagnet and Allemand, 2020, Simpson

501 et al., 2020) or for the resuspension of particles generated by vehicles (Amato et al., 2014). On
502 the other hand the spatial allocation for emissions can be uncertain for some sectors. These
503 lacking or incomplete emission sources will lead to a potential ~~underestimation~~ misestimate of
504 the city responsibility ~~as well~~.

505
506 On the meteorological side, the estimation of wind speed, PBL height and/or turbulence intensity
507 will largely influence the dispersion of city emissions and uncertainties in these will therefore
508 impact the calculation of city contributions. While the impact of meteorological parameterization
509 on air quality has been extensively assessed from regional to urban cases (De Meij et al., 2009;
510 (De Meij et al. 2015; De Meij et al. 2018; Jiang et al., 2020), only few studies assessed their
511 importance on city contributions. One of these (Huszar et al. 2021) shows e.g. that the inclusion
512 of an urban canopy meteorological forcing on multi-year simulations largely impacts the
513 estimation of the city responsibility.

514
515 In the next section, we discuss the consequences of these results on policy, in particular when SA
516 information is used to design air quality plans.

517 4. Implications for air quality strategies

518 Estimating the contribution of a city to its pollution has important consequences in terms of air
519 quality management. Indeed, an important city contribution will be a logic argument to support
520 substantial control measures at the local level to abate pollution. The effectiveness of the control
521 measures then relies on the relevance and accuracy of this city contribution; over- or under-
522 estimated city contributions potentially leading to inefficient measures.

523 In previous sections, we have seen that the city contribution largely varies depending on the
524 choices made for the SA setting parameters (definition of the indicator, source, receptor and
525 methodology), hence the challenge to obtain a relevant and accurate estimate to support local
526 action.

527 Given the range of possible SA options and their impact on results, the first recommendation is
528 obviously to report these SA setting choices together with the results to provide policymakers
529 with the full picture and allow them to take informed decisions. This advocates for the use of the
530 proposed nomenclature or a similar one that documents for the choices in the SA approach,
531 providing accountability to the method and enabling correct interpretation of the results. The
532 proposed nomenclature can be understood as a documentation of the SA metadata information.
533 Apart from this point on the importance of documenting SA approach choices, we show below
534 that some of the SA settings are fixed by the purpose of the study. We provide suggestions for
535 the remaining free choices.

536 The recommended SA method is potential impacts (PI)

537
538
539 It is important to recall that not all SA methodologies are equally suited to support air quality
540 planning. As mentioned by several authors (Burr and Zhang 2011, Qiao et al. 2018, Mertens et
541 al. 2019, Clappier et al. 2017, Grewe et al. 2010, 2012; Thunis et al. 2019), potential impacts are
542 recommended when non-linear species are involved (which is the case for PM_{2.5} and PM₁₀ but
543 also for other species like NO₂ or O₃). It is worth reminding that tagging or incremental
544 approaches are yet erroneously used and believed to be suited for air quality planning purposes
545 (Qiao et al. 2018; Guo et al. 2017; Itahashi et al. 2017; Timmermans et al. 2017; Wang et al.

Formatted: Not Highlight

Formatted: Not Highlight

Formatted: Not Highlight

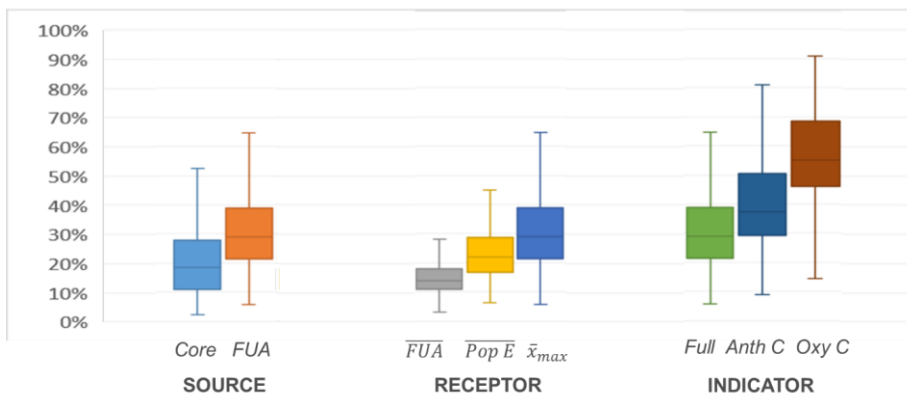
Formatted: Not Highlight

Formatted: Not Highlight

Formatted: Not Highlight

546 2015, Hendriks et al. 2013). Although challenging practical issues are attached to potential
 547 impacts and may be seen as a burden (e.g. lack of additivity, see Appendix), they only reflect the
 548 complexity of the real processes that must be accounted for. ~~Although It is true that~~ uncertainties
 549 associated to the PI approach (e.g. imperfect emission inventory), may lead other SA methods to
 550 perform better in some instances because methodological biases compensate uncertainties, this is
 551 however coincidental. While uncertainties can be tackled and reduced to improve the approach,
 552 this is not the case of methodological biases. These points ~~were~~ are extensively discussed in
 553 Thunis et al. (2019).

554
 555 For the remaining of this section focusing on policy aspects, only potential impact results are
 556 discussed. Fixing the methodology however still leaves free options in terms of indicator,
 557 receptor and source. This is visualized in Figure 8 that summarizes the variability of the SA
 558 results presented in the previous sections (i.e. Figure 2, Figure 4 and Figure 6) for the 150 cities
 559 to these possible choices. Differences in terms of city responsibility reach a factor 2 in average
 560 for each of these remaining parameters with much larger values for some cities.
 561



562
 563 *Figure 8: Box quantile diagrams summarizing the city contributions to PM_{2.5} levels for the 150 EU cities. All results are based on*
 564 *a similar method (potential impacts at 50%), a similar temporal receptor (\bar{Y}) but for different choices of city sources (left),*
 565 *receptors (centre) and indicators (right). See previous sections for details. The two extremities of each vertical line represent the*
 566 *10th and 90th percentile contributions among the 150 cities, respectively. The box crossing horizontal line represents the median.*

567
 568 **INDICATOR: The indicator choice is driven by health and environmental objectives**
 569

570 The choice of the indicator is generally motivated by health or environmental considerations.
 571 Currently, the WHO guidelines (WHO2005) refer to the total PM_{2.5} mass as the indicator
 572 correlating best with health impacts. These guidelines (or the AAQD limit values) are then the
 573 logical and most relevant indicator choice among the options presented in Section 3.1 and shown
 574 in Figure 2. As illustrated by Figure 8, evolving knowledge on health-related pollution impacts
 575 (i.e. the increased toxicity of some PM_{2.5} constituents like those related to the traffic and
 576 residential activities) might however, drive the choice towards more detailed indicators (e.g.
 577 PPM_{2.5}) leading to an increased responsibility for the cities.
 578

579 SOURCE: Importance of matching sources with governance levels

580
581 Figure 8 shows that plans limited to city cores would be significantly less efficient than if applied
582 at the FUA scale. In average over all cities, the efficiency decreases by a factor 2 but larger
583 differences occur in many cities. The source does however not represent a free choice in the
584 context of policy practice. Indeed, authorities in charge of AQ plans only have power to act on
585 the area under their responsibility, which sets where measures apply. The same applies for the
586 source temporal characteristic, fixed as the period of time during which measures apply. A good
587 match between the SA settings and the temporal and spatial characteristics of the source is
588 therefore important to provide meaningful support to policy makers.

589
590 RECEPTOR: Drawbacks associated to spatial and temporal averaging processes at the receptor

591
592 As clearly shown in Figure 5, spatial averaging processes lead to a loss of information. In our
593 example, a city average based SA would totally occult the city center SA. It would lead to a
594 strategy that mostly targets the background at the expense of the city center, where the high
595 concentration issues would not be solved. This is well illustrated by Amann et al. (2017) who
596 ~~analyse~~analyze the responsibility of the city of New Delhi on its air pollution, both at a city
597 center hot-spot receptor and in terms of city average population exposure. In the first case, SA
598 suggests acting on local sources while in the second SA suggests acting on regional sources.
599 Spatial averaging drives the balance towards regional actions that will be less effective in solving
600 the pollution issue at the city center.- The larger the city, the more important this shift will be. As
601 illustrated by Figure 8, there is more than a factor 2 between city-averaged and hot spot
602 indicators. Similar considerations apply to temporal averages.- Figure 7 clearly shows that yearly
603 average values hide the potential for effective local actions during wintertime and even more on
604 specific days.

605
606 Averaging implies merging, into one single number, locations and time instants that are
607 characterized by different and sometimes opposite SA. This may lead to strategies that will not
608 be efficient everywhere all the time. Whenever the final objective is to reduce a temporally
609 or/and spatially averaged indicator (e.g. average population exposure), strategies would gain in
610 efficiency with the following process: (1) perform SA and hierarchize the raw (not averaged) SA
611 results into homogeneous spatio-temporal clusters; (2) design strategies on the basis of these
612 clusters; (3) assess the strategy efficiency against the averaged indicator. The key is here to
613 design strategies on raw or clustered results rather than on averaged ones, to prevent information
614 loss.

615
616 Note that designing a unique strategy based on multiple SA results (point 2 above) does not
617 necessarily complicate the analysis, as these different SA will likely suggest action on different
618 sectors of activity that can be combined ~~at~~in the final strategy.

619

620 5. Conclusions

621 Although air quality has improved in Europe over the last decades, in great part thanks to
622 effective measures and consistent EU-wide legislation, pollution hot spots yet remain in many
623 European cities. The extent by which city emissions are causing these elevated urban pollution

624 levels is however still a subject of scientific discussion. This can be explained by the complex
625 processes driving the formation of some pollutants like PM_{2.5}, for which there is not a simple
626 relationship between emissions and concentrations (in other words, local emissions don't always
627 imply local responsibilities). Source apportionment represents a useful technique to quantify the
628 city responsibility but the approaches and applications are however not harmonized, therefore
629 not comparable, resulting in confusing and sometimes contradicting interpretations.

Formatted: Subscript

630 In this work, we analyzed how different SA approaches apply to the urban scale and how their
631 building elements and parameters are defined and set. We identified the possible settings
632 associated to four key steps in SA: indicator, receptor, source and methodology. We showed that
633 different choices for these settings lead to very large differences in terms of results. In average
634 over the 150 European large cities selected as example, the choices made for the indicator, the
635 receptor, and the source each lead to an average factor 2 difference in terms of city
636 responsibility. These various options and the large differences that result, highlight the difficulty
637 of comparing results from different studies and stress the need to document the SA approach
638 with its related metadata – that documents details the choices made for the key four steps.
639

640 This work advocates for the use of a harmonized nomenclature to support the comparability of
641 SA approaches. We propose the use of indexes and sub-indexes attached to the 4 key steps in any
642 SA approach in a harmonized way to uniquely document the approach and enable correct
643 interpretation of the results. We believe that the adoption of this nomenclature will provide
644 clarity to the scientific discussion on different results and enable the correct interpretation of the
645 results for policy applications. Even though this is applied to the specific case of PM_{2.5}, the
646 concepts presented here can easily be generalized to other pollutants.
647

648 In the context of supporting urban air quality plans, the SA configuration and most setting
649 parameters are driven by the purpose of the AQ plan itself and by its associated constraints.
650 While environmental and/or health related considerations guide the choice of the indicator, the
651 spatio-temporal characteristics of the source are strongly correlated to governance aspects. In
652 other words, the source characteristics should reflect the governance levels to facilitate
653 interpretation. Finally, the recommended SA method should be based on “potential impacts”, to
654 prevent misleading interpretations in terms of expected AQ plan outcome.
655

656 At the receptor level, temporal and spatial averaging processes lead to a loss of information,
657 especially when diverging SA results are aggregated into a single number. Averaging process, in
658 particular spatial, often lead to favor strategies that target background sources while neglecting
659 actions that would be efficient at the city center. In our 150 cities example, the impact of spatial
660 averaging leads to an average factor 2 difference in terms of city responsibility. Not only results
661 differ from one city to the other, and from one location to another in a given city, they also differ
662 through time. To cope with this variability, we recommend using non-averaged SA results for the
663 design of AQ strategies. Once clustered in homogeneous spatio-temporal classes, these can serve
664 to understand where and when actions are most efficient. When implemented, the efficiency of
665 abatement measures can then be assessed via spatially and temporally averaged indicator (e.g.
666 city average population exposure).
667
668

669 The responsibility of a city to its pollution is obviously city dependent. But even for a given city,
670 SA studies using different approaches and parameter settings will deliver very different
671 outcomes. It is important to note that a departure from the methodological recommendations
672 listed above, additional uncertainties and assumptions will most often lead to a systematic and
673 important underestimation of the city responsibility. We showed that in average over 150
674 European cities, departures in terms of source, receptor, and indicator may lead for each to a
675 factor 2 underestimation. This comes with important implications: if cities are seen as a minor
676 actor, plans will target in priority the background at the expense of potentially effective local
677 actions.

678
679 Future work will consist in comparing spatially/temporally averaged SA results with SA results
680 that are clustered in homogeneous spatio-temporal classes and assess the implications in terms of
681 AQ strategy.

682 683 Acknowledgements

684 The Authors thank Chloé Thunis for her support [in adapting some 'Flaticon.com' images to](#)
685 [ourwith the infographics needs.](#)

686 687 688 References

- 689 Alberti, V., Alonso Raposo, M., Attardo, C., Auteri, D., Ribeiro Barranco, R., Batista E Silva, F.,
690 Benczur, P., Bertoldi, P., Bono, F., Bussolari, I., Louro Caldeira, S., Carlsson, J.,
691 Christidis, P., Christodoulou, A., Ciuffo, B., Corrado, S., Fioretti, C., Galassi, M.,
692 Galbusera, L., Gawlik, B., Giusti, F., Gomez Prieto, J., Grosso, M., Martinho Guimaraes
693 Pires Pereira, A., Jacobs, C., Kavalov, B., Kompil, M., Kucas, A., Kona, A., Lavallo, C.,
694 Leip, A., Lyons, L., Manca, A., Melchiorri, M., Monforti-Ferrario, F., Montalto, V.,
695 Mortara, B., Natale, F., Panella, F., Pasi, G., Perpia Castillo, C., Pertoldi, M., Pisoni, E.,
696 Roque Mendes Polvora, A., Rainoldi, A., Rembges, D., Rissola, G., Sala, S., Schade, S.,
697 Serra, N., Spirito, L., Tsakalidis, A., Schiavina, M., Tintori, G., Vaccari, L., Vandyck, T.,
698 Vanham, D., Van Heerden, S., Van Noordt, C., Vespe, M., Veters, N., Vilahur
699 Chiaraviglio, N., Vizcaino, M., Von Estorff, U. and Zulian, G., The Future of Cities,
700 Vandecasteele, I., Baranzelli, C., Siragusa, A. and Aurambout, J. editor(s), EUR 29752
701 EN, Publications Office of the European Union, Luxembourg, 2019, ISBN 978-92-76-
702 03847-4, doi:10.2760/375209, JRC116711.
- 703 Amann, M., Pallav Purohit, Anil D. Bhanarkar, Imrich Bertok, Jens Borcken-Kleefeld, Janusz
704 Cofala, Chris Heyes, Gregor Kiesewetter, Zbigniew Klimont, Jun Liu, Dipanjali
705 Majumdar, Binh Nguyen, Peter Rafaj, Padma S. Rao, Robert Sander, Wolfgang Schöpp,
706 Anjali Srivastava, B. Harsh Vardhan, 2017. Managing future air quality in megacities: A
707 case study for Delhi, Atmospheric Environment, 161, 99-111.
- 708 AQD, 2008. Directive 2008/50/EC of the European Parliament and of the Council of 21 May
709 2008 on ambient air quality and cleaner air for Europe (No. 152). Official Journal.
- 710 Amato, F., Cassee, F.R., Denier van der Gon, H.A.C., Gehrig, R., Gustafsson, M., Hafner, W.,
711 Harrison, R.M., Jozwicka, M., Kelly, F.J., Moreno, T., Prevot, A.S.H., Schaap, M.,
712 Sunyer, J., Querol, X., 2014. Urban air quality: The challenge of traffic non-exhaust
713 emissions. Journal of Hazardous Materials 275, 31–36.
714 <https://doi.org/10.1016/j.jhazmat.2014.04.053>

715 ATMO2003: L'indice ATMO: indicateur de la qualité de l'air dans les agglomérations françaises
716 [The ATMO index: an air quality indicator for developed areas in France]. *Eur Ann*
717 *Allergy Clin Immunol.* 2003 May;35(5):166-9. French. PMID: 12838780.

718 ApSimon H., T. Oxley, H. Woodward, D. Mehlig, A. Dore, M. Holland, 2021. The UK
719 Integrated Assessment Model for source apportionment and air pollution policy
720 applications to PM2.5, *Environment International*, 153, 106515.

721 Belis, C.A., D. Pernigotti, G. Pirovano, O. Favez, J.L. Jaffrezo, J. Kuenen, H. Denier van Der
722 Gon, M. Reizer, V. Riffault, L.Y. Alleman, M. Almeida, F. Amato, A. Angyal, G.
723 Argyropoulos, S. Bande, I. Beslic, J.-L. Besombes, M.C. Bove, P. Brotto, G. Calori, D.
724 Cesari, C. Colombi, D. Contini, G. De Gennaro, A. Di Gilio, E. Diapouli, I. El Haddad,
725 H. Elbern, K. Eleftheriadis, J. Ferreira, M. Garcia Vivanco, S. Gilardoni, B. Golly, S.
726 Hellebust, P.K. Hopke, Y. Izadmanesh, H. Jorquera, K. Krajsek, R. Kranenburg, P.
727 Lazzeri, F. Lenartz, F. Lucarelli, K. Maciejewska, A. Manders, M. Manousakas, M.
728 Masiol, M. Mircea, D. Mooibroek, S. Nava, D. Oliveira, M. Paglione, M. Pandolfi, M.
729 Perrone, E. Petralia, A. Pietrodangelo, S. Pillon, P. Pokorna, P. Prati, D. Salameh, C.
730 Samara, L. Samek, D. Saraga, S. Sauvage, M. Schaap, F. Scotto, K. Sega, G. Siour, R.
731 Tauler, G. Valli, R. Vecchi, E. Venturini, M. Vestenius, A. Waked, E. Yubero, 2020.
732 Evaluation of receptor and chemical transport models for PM10 source apportionment,
733 *Atmospheric Environment: X*, 5,100053.

734 Bhave P.V., Pouliot G.A. and Zheng M., 2007. Diagnostic model evaluation for carbonaceous
735 PM2.5 using organic markers measured in the southeastern U.S. *Environmental Science*
736 *and Technology* 41, 1577-1583.

737 Burr M.J. and Y. Zhang, 2011b. Source apportionment of fine particulate matter over the Eastern
738 U.S. Part II: source sensitivity simulations using CAMX/PSAT and comparisons with
739 CMAQ source sensitivity simulations, *Atmospheric Pollution Research*, 2, 318-336

740 Clappier A., E. Pisoni, P.Thunis, 2015. A new approach to design source–receptor relationships
741 for air quality modelling. *Environmental Modelling & Software*, 74, 66-74.

742 Clappier A., C. Belis, D. Pernigotti and P. Thunis (2017) Source apportionment and sensitivity
743 analysis: two methodologies with two different purposes. *Geosci. Model Dev. Discuss.*,
744 <https://doi.org/10.5194/gmd-2017-161>, in review, 2017.

745 de Bruyn, S., de Vries, J., 2020. Health costs of air pollution in European cities and the linkage
746 with transport (No. 20.190272.134). CE Delft, Delft.

747 Degraeuwe, B., Pisoni, E., Peduzzi, E., De Meij, A., Monforti-Ferrario, F., Bodis, K.,
748 Mascherpa, A., Astorga-Llorens, M., Thunis, P. and Vignati, E., *Urban NO2 Atlas, EUR*
749 *29943 EN*, Publications Office of the European Union, Luxembourg, 2019, ISBN 978-
750 92-76-10386-8 (online),978-92-76-10387-5 (print), doi:10.2760/43523
751 (online),10.2760/538816 (print), JRC118193.

752 De Meij, A., S. Wagner, N. Gobron, P. Thunis, C. Cuvelier, F. Dentener, M. Schaap, Model
753 evaluation and scale issues in chemical and optical aerosol properties over the greater
754 Milan area (Italy), for June 2001, *Atmos. Res.* 85, 243-267, 2007.

755 De Meij, A., Gzella, A., Cuvelier, C., Thunis, P., Bessagnet, B., Vinuesa, J.F., Menut, L., Kelder,
756 H.M., 2009. The impact of MM5 and WRF meteorology over complex terrain on
757 CHIMERE model calculations. *Atmospheric Chemistry and Physics* 9, 6611–6632.

758 De Meij, A., Bossioli, E., Vinuesa, J.F., Penard, C., Price, I., The effect of SRTM and Corine
759 Land Cover on calculated gas and PM10 concentrations in WRF-Chem. *Atmos. Env.*
760 Volume 101, Pages 177–193, January 2015.

Formatted: French (France)

761 [De Meij, A., Zittis, G. & Christoudias, T.: On the uncertainties introduced by land cover data in](#)
762 [high-resolution regional simulations, Meteorol. Atmos. Phys. \(2018\).](#)
763 <https://doi.org/10.1007/s00703-018-0632-3>; <https://rdcu.be/38pt>
764
765 European Environment Agency. Air Quality in Europe: 2020 Report. Publications Office, 2020.
766 DOI.org (CSL JSON), <https://data.europa.eu/doi/10.2800/786656>.
767 European Environment Agency, Air quality in Europe — 2017 report, No13/2017, ISSN 1977-
768 8449, doi:10.2800/850018, [https://www.eea.europa.eu/publications/air-quality-in-europe-](https://www.eea.europa.eu/publications/air-quality-in-europe-2017)
769 2017.
770 European Commission. Joint Research Centre. Institute for Energy and Transport., 2014. Non-
771 exhaust traffic related emissions - Brake and tyre wear PM: literature review.
772 Publications Office, LU.
773 Grewe, V., E. Tsati, P. Hoor, 2010. On the attribution of contributions of atmospheric trace gases
774 to emissions in atmospheric model applications, Geosci. Model Dev., 3, 487-499
775 Grewe, V., K. Dahlmann, S. Matthes, W. Steinbrecht, 2012. Attributing ozone to NOx
776 emissions: Implications for climate mitigation measures, Atmos. Environ., 59, 102-107
777 Guo H., S. H. Kota, S. K. Sahu, J. Hu, Q. Ying, A. Gao, H. Zhang, 2017. Source apportionment
778 of PM2.5 in North India using source-oriented air quality models. Environmental
779 Pollution 231, 426-436.
780 Hendriks C., R. Kranenburg, J. Kuenen, R. van Gijlswijk, R. Wichink Kruit, A. Segers, H.
781 Denier van der Gon, M. Schaap, 2013. The origin of ambient particulate matter
782 concentrations in the Netherlands, Geosci. Model Dev., 6, 721–733, 2013
783 Huang Y., T. Deng, Z. Li, N. Wang, C. Yin, S. Wang, S. Fan, 2018. Numerical simulations for
784 the sources apportionment and control strategies of PM2.5 over Pearl River Delta, China,
785 part I: Inventory and PM2.5 sources apportionment, Science of the Total Environment
786 634 (2018) 1631–1644.
787 [Huszar, P., Belda, M., and Halenka, T.: On the long-term impact of emissions from central](#)
788 [European cities on regional air quality, Atmos. Chem. Phys., 16, 1331–1352,](#)
789 <https://doi.org/10.5194/acp-16-1331-2016>, 2016
790 [Huszar, P., Karlický, J., Marková, J., Nováková, T., Liaskoni, M., and Bartík, L.: The regional](#)
791 [impact of urban emissions on air quality in Europe: the role of the urban canopy effects,](#)
792 [Atmos. Chem. Phys. \[preprint\], https://doi.org/10.5194/acp-2021-355, accepted for final](#)
793 [publication, 2021.](#)
794 Itahashi S., H. Hayami, K. Yumimoto, I. Uno, 2017. Chinese province-scale source
795 apportionments for sulfate aerosol in 2005 evaluated by the tagged tracer method,
796 Environmental Pollution 220, 1366-1375.
797 [Jiang, L., Bessagnet, B., Meleux, F., Tognet, F., Couvidat, F., 2020. Impact of physics](#)
798 [parameterizations on high-resolution air quality simulations over the Paris region.](#)
799 [Atmosphere 11.](#)
800
801 Kaspar R. Daellenbach, Gaëlle Uzu, Jianhui Jiang, Laure-Estelle Cassagnes, Zaira Leni,
802 Athanasia Vlachou, Giulia Stefanelli, Francesco Canonaco, Samuël Weber, Arjo Segers,
803 Jeroen J. P. Kuenen, Martijn Schaap, Olivier Favez, Alexandre Albinet, Sebnem
804 Aksoyoglu, Josef Dommen, Urs Baltensperger, Marianne Geiser, Imad El Haddad, Jean-
805 Luc Jaffrezo, André S. H. Prévôt. Sources of particulate-matter air pollution and its

806 oxidative potential in Europe. *Nature*, 2020; 587 (7834): 414 DOI: 10.1038/s41586-020-
807 2902-8

808 Keuken M., M. Moerman, M. Voogt, M. Blom, E.P. Weijers, T. Röckmann, U. Dusek (2013)
809 Source contributions to PM_{2.5} and PM₁₀ at an urban background and a street location,
810 *Atmos. Environ.*, 71, 26–35.

811 Khomenko, S., Cirach, M., Pereira-Barboza, E., Mueller, N., Barrera-Gómez, J., Rojas-Rueda,
812 D., de Hoogh, K., Hoek, G., Nieuwenhuijsen, M., 2021. Premature mortality due to air
813 pollution in European cities: a health impact assessment. *The Lancet Planetary Health*
814 S2542519620302722. [https://doi.org/10.1016/S2542-5196\(20\)30272-2](https://doi.org/10.1016/S2542-5196(20)30272-2)

815 Kieseewetter G. and Amann (2014). Urban PM_{2.5} levels under the EU Clean Air Policy Package,
816 IIASA TSAP Report 12.

817 Kieseewetter G., J. Borcken-Kleefeld, W. Schöpp, C. Heyes, P. Thunis, B. Bessagnet, E.
818 Terrenoire, H. Fagerli, A. Nyiri and M. Amann (2015) Modelling street level PM₁₀
819 concentrations across Europe: source apportionment and possible futures, *Atmos. Chem.*
820 *Phys.*, 15, 1539-1553.

821 Kranenburg R., Segers A., Hendriks C., and Schaap,. 2013. Source apportionment using
822 LOTOS-EUROS: module description and evaluation, *Geosci. Model Dev.*, 6, 721–733

823 Kole, P.J., Löhr, A.J., Van Bellegem, F., Ragas, A., 2017. Wear and Tear of Tyres: A Stealthy
824 Source of Microplastics in the Environment. *IJERPH* 14, 1265.
825 <https://doi.org/10.3390/ijerph14101265>

826 Kwok R.H.F., S.L. Napelenok, K.R. Baker, 2013: Implementation and evaluation of PM_{2.5}
827 source contribution analysis in a photochemical model, *Atmospheric Environment* 80,
828 398-407

829 Lavallo, C., Pontarollo, N., Batista E Silva, F., Baranzelli, C., Jacobs, C., Kavalov, B., Kompil,
830 M., Perpiña Castillo, C., Vizcaino, M., Ribeiro Barranco, R., Vandecasteele, I., Pinto
831 Nunes Nogueira Diogo, V., Aurambout, J., Serpieri, C., Marín Herrera, M., Rosina, K.,
832 Ronchi, S. and Auteri, D., *European Territorial Trends - Facts and Prospects for Cities*
833 *and Regions* Ed. 2017, EUR 28771 EN, Publications Office of the European Union,
834 Luxembourg, 2017, ISBN 978-92-79-79906-8, doi:10.2760/28183, JRC107391.

835 Lenschow P., H.-J. Abraham, K. Kutzner, M. Lutz, J.-D. Preu, W. Reichenbacher (2001) Some
836 ideas about the sources of PM₁₀, *Atmospheric Environment* 35 Supplement No. 1 23–33.

837 Li Y., D. K. Henze, D. Jack, B. H. Henderson, P. L. Kinney, 2016. Assessing public health
838 burden associated with exposure to ambient black carbon in the United States, *Science of*
839 *the Total Environment* 539, 515–525.

840 Fei Liu, Z. Klimont, Qiang Zhang, J. Cofala, Lijian Zhao, Hong Huo, B. Nguyen, W. Schöpp, R.
841 Sander, Bo Zheng, Chaopeng Hong, Kebin He, M. Amann, Ch. Heyes, 2013. Integrating
842 mitigation of air pollutants and greenhouse gases in Chinese cities: development of
843 GAINS-City model for Beijing, *Journal of Cleaner Production*, Volume 58, 25-33,
844 <https://doi.org/10.1016/j.jclepro.2013.03.024>.

845 Luo H., L. Yang, Z. Yuan, K. Zhao, S. Zhang, Y. Duan, R. Huang, Q. Fu, 2020. Synoptic
846 condition-driven summertime ozone formation regime in Shanghai and the implication
847 for dynamic ozone control strategies, *Science of The Total Environment*, 745, 141130.

848 Mertens, M., Volker G., V.S. Rieger and P. Jöckel. Revisiting the contribution of land transport
849 and shipping emissions to tropospheric ozone, *Atmos. Chem. Phys.*, 18, 5567–5588, 2018

850 Ntziachristos, L., Boulter, P., 2019. EMEP/EEA air pollutant emission inventory guidebook
851 2019 - 1.A.3.b.vi Road transport: Automobile tyre and brake wear - 1.A.3.b.vii Road
852 transport: Automobile road abrasion. European Environment Agency.

853 OECD (2012) Redefining Urban: a new way to measure metropolitan areas, OECD report,
854 ISBN: 9789264174054, 148pp.

855 O'Neill, B. C., Dalton, M., Fuchs, R., Jiang, L., Pachauri, S., Zigova, K., Global demographic
856 trends and future carbon emissions, Proceedings of the National Academy of Sciences
857 Oct 2010, 107 (41) 17521-17526; DOI: 10.1073/pnas.1004581107.

858 Ortiz S. and Friedrich, R.: A modelling approach for estimating background pollutant
859 concentrations in urban areas, Atmos. Pollut. Res., 4, 147–156,
860 doi:10.5094/APR.2013.015, 2013.

861 Osada, K., Ohara, T., Uno, I., Kido, M., Iida, H., 2009. Impact of Chinese anthropogenic
862 emissions on submicrometer aerosol concentration at Mt. Tateyama, Japan. Atmos.
863 Chem. Phys. 9 (23), 9111–9120.

864 Park, M., Joo, H.S., Lee, K. et al. Differential toxicities of fine particulate matters from various
865 sources. Sci Rep 8, 17007 (2018). <https://doi.org/10.1038/s41598-018-35398-0>

866 Petetin H. M. Beekmann, J. Sciare, M. Bressi, A. Rosso, O. Sanchez and V. Ghers. (2014) A
867 novel model evaluation approach focusing on local and advected contributions to urban
868 PM2.5 levels – application to Paris, France, Geosci. Model Dev., 7, 1483–1505.

869 Pey J., X. Querol and A. Alastuey, 2010, Discriminating the regional and urban contributions in
870 the North-Western Mediterranean: PM levels and composition, Atmospheric
871 Environment 44, 1587-1596.

872 Pisoni E., A. Clappier, B. Degraeuwe, P. Thunis, 2017. Adding spatial flexibility to source-
873 receptor relationships for air quality modelling, Environmental Modelling & Software,
874 90, 68-77.

875 [Pisoni et al. 2021. A new methodology to evaluate the effectiveness of local policies during high](#)
876 [PM2.5 episodes: application on 10 European cities. Submitted to ACP](#)

877 Pommier, M., Fagerli, H., Schulz, M., Valdebenito, A., Kranenburg, R., and Schaap, M.:
878 Prediction of source contributions to urban background PM10 concentrations in European
879 cities: a case study for an episode in December 2016 using EMEP/MSC-W rv4.15 and
880 LOTOS-EUROS v2.0 – Part 1: The country contributions, Geosci. Model Dev., 13,
881 1787–1807, <https://doi.org/10.5194/gmd-13-1787-2020>, 2020.

882 Qiao X., Q. Ying, X. Li, H. Zhang, J. Hu, Y. Tang, X. Chen, 2018. Source apportionment of
883 PM2.5 for 25 Chinese provincial capitals and municipalities using a source-oriented
884 Community Multiscale Air Quality model, Science of the Total Environment 612, 462–
885 471.

886 Raifman, M., Russell, A. G., Skipper, T. N., & Kinney, P. L. (2020). Quantifying the health
887 impacts of eliminating air pollution emissions in the city of Boston. Environmental
888 Research Letters, 15(9) doi:10.1088/1748-9326/ab842b

889 Schaap, M., Timmermans, R.M.A., Roemer, M., Boersen, G.A.C., Builtjes, P.J.H. Sauter, F.J.,
890 Velders, G.J.M. and Beck, J.P. (2008) 'The LOTOS-EUROS model: description,
891 validation and latest developments', Int. J. Environment and Pollution, Vol. 32, No. 2,
892 pp.270–290.

893 Simpson, D., Benedictow, A., Berge, H., Bergström, R., Emberson, L. D., Fagerli, H., Flechard,
894 C. R., Hayman, G. D., Gauss, M., Jonson, J. E., Jenkin, M. E., Nyíri, A., Richter, C.,
895 Semeena, V. S., Tsyro, S., Tuovinen, J.-P., Valdebenito, Á., and Wind, P.: The EMEP

896 MSC-W chemical transport model – technical description, *Atmos. Chem. Phys.*, 12,
897 7825–7865, <https://doi.org/10.5194/acp-12-7825-2012>, 2012.

898 Squizzato S. and M. Masiol (2015) Application of meteorology-based methods to determine
899 local and external contributions to particulate matter pollution: A case study in Venice
900 (Italy), *Atmospheric Environment* 119, 69-81.

901 Timmermans R.M.A., H.A.C. Denier van der Gon, J.J.P. Kuenen, A.J. Segers, C. Honoré, O.
902 Perrussel, P.J.H. Builtjes and M. Schaap (2013) Quantification of the urban air pollution
903 increment and its dependency on the use of down-scaled and bottom-up city emission
904 inventories, *Urban Climate* 6, 44–62.

905 UN, 2020 Policy Brief, Covid-19 in an urban world.
906 [https://www.un.org/sites/un2.un.org/files/sg_policy_brief_covid_urban_world_july_2020](https://www.un.org/sites/un2.un.org/files/sg_policy_brief_covid_urban_world_july_2020.pdf)
907 .pdf

908 Thunis, P., Degraeuwe, B., Peduzzi, E., Pisoni, E., Trombetti, M., Vignati, E., Wilson, J., Belis,
909 C. and Pernigotti, D., *Urban PM2.5 Atlas: Air Quality in European cities*, EUR 28804
910 EN, Publications Office of the European Union, Luxembourg, 2017, ISBN 978-92-79-
911 73876-0 (online),978-92-79-73875-3 (print),978-92-79-75274-2 (ePub),
912 doi:10.2760/336669 (online),10.2760/851626 (print),10.2760/865663 (ePub),
913 JRC108595.

914 Thunis P. (2018). On the validity of the incremental approach to estimate the impact of cities on
915 air quality, *Atmospheric Environment*, 173, 210-222.

916 Thunis P., B. Degraeuwe, E. Pisoni, M. Trombetti, E. Peduzzi, C.A. Belis, J. Wilson, A.
917 Clappier, E. Vignati, 2018. PM2.5 source allocation in European cities: A SHERPA
918 modelling study, *Atmospheric Environment*, 187, 93-106.

919 Tobías, A., Carnerero, C., Reche, C., Massagué, J., Via, M., Minguillón, M. C., . . . Querol, X.
920 202). Changes in air quality during the lockdown in barcelona (spain) one month into the
921 SARS-CoV-2 epidemic. *Science of the Total Environment*, 726
922 doi:10.1016/j.scitotenv.2020.138540

923 Transboundary particulate matter, photo-oxidants, acidification and eutrophication components.
924 Joint MSC-W & CCC & CEIP Report. EMEP Status Report 1/2017

925 United Nations, Department of Economic and Social Affairs, Population Division (2018), *The*
926 *World's Cities in 2018 – Data Booklet (ST/ESA/SER.A/417)*.

927 Van Dingenen R., F. Dentener, M. Crippa, J. Leitao, E. Marmer, S. Rao, E. Solazzo and L.
928 Valentini, 2018. TM5-FASST: a global atmospheric source-receptor model for rapid
929 impact analysis of emission changes on air quality and short-lived climate pollutants.
930 *Atmospheric Chemistry and Physics*, <https://doi.org/10.5194/acp-2018-112>

931 Viana, M., Querol, X., Alastuey, A., Ballester, F., Llop, S., Esplugues, A., . . . Herte, M. D.
932 (2008). Characterising exposure to PM aerosols for an epidemiological study.
933 *Atmospheric Environment*, 42(7), 1552-1568. doi:10.1016/j.atmosenv.2007.10.087

934 Wagstrom, K. M., Pandis, S. N., Yarwood, G., Wilson, G. M., and Morris, R. E., 2008:
935 Development and application of a computationally efficient particulate matter
936 apportionment algorithm in a three dimensional chemical transport model, *Atmos.*
937 *Environ.*, 42, 5650–5659.

938 Wang Z. S., Chien C.-J., and Tonnesen G. S., 2009. Development of a tagged species source
939 apportionment algorithm to characterize three-dimensional transport and transformation
940 of precursors and secondary pollutants, *J. Geophys. Res.*, 114, D21206

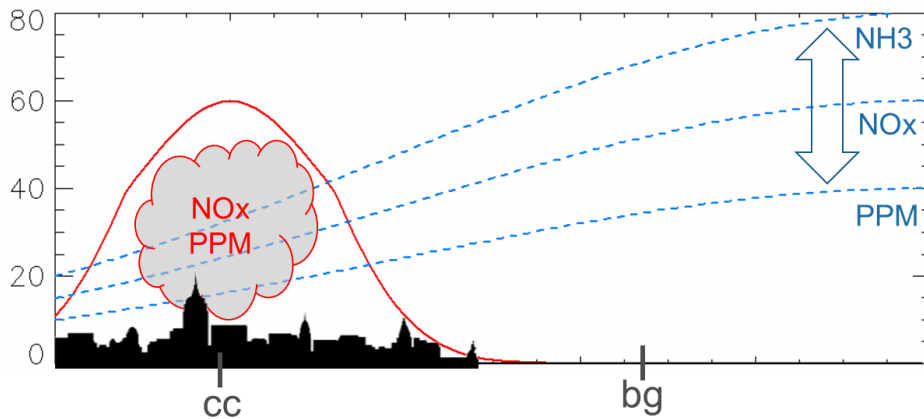
- 941 Wang L., Z. Wei, W. Wei, J. S. Fu, C. Meng, S. Ma, 2015. Source apportionment of PM2.5 in
942 top polluted cities in Hebei, China using the CMAQ model, *Atmospheric Environment*
943 122, 723-736
- 944 Wang, L.T., Wei, Z., Yang, J., Zhang, Y., Zhang, F.F., Su, J., Meng, C.C., Zhang, Q., 2014. The
945 2013 severe haze over southern Hebei, China: model evaluation, source apportionment,
946 and policy implications. *Atmos. Chem. Phys.* 14, 3151-3173.
- 947 WHO2005, *Air Quality Guidelines Global Update 2005. Particulate matter, ozone, nitrogen*
948 *dioxide and sulfur dioxide*, ISBN 92 890 2192 6
- 949 Wu, Q.Z., Wang, Z.F., Gbaguidi, A., Gao, C., Li, L.N., Wang, W., 2011. A numerical study of
950 contributions to air pollution in Beijing during CAREBeijing-2006. *Atmos. Chem. Phys.*
951 11 (12), 5997–6011.
- 952 Yarwood G., Morris R.E., and Wilson G.M., 2004. *Particulate Matter Source Apportionment*
953 *Technology (PSAT) in the CAMx Photochemical Grid Model. Proceedings of the 27th*
954 *NATO/ CCMS International Technical Meeting on Air Pollution Modeling and*
955 *Application.* Springer Verlag
956

957 Appendix A

958 To illustrate the differences among SA methods, we use here the theoretical example
 959 schematically represented in Figure A1. -A city source (in red) emits with a Gaussian dispersion
 960 profile both primary PM (PPM) and a gas-phase precursor (NO_x). The background pollution (in
 961 blue) is composed of a mix of NO_x, NH₃ and PPM compounds. The various chemical reactions
 962 that take place are simplified here for convenience into a single reaction. One mole of NH₃ reacts
 963 with one mole of NO_x to create one mole of ammonium nitrate (NH₄⁺NO₃⁻), i.e. secondary PM.
 964 (NO_x + NH₃ + X →→ NH₄⁺NO₃⁻). We assume here that the external compounds involved in the
 965 reaction (X) are abundant and do not have a limiting effect on the formation of PM. While the
 966 city emissions (source) remain unchanged, we modify the relative importance of the three
 967 background compounds so that the background becomes in turn PPM, NO_x and NH₃ dominated.
 968 The PM concentration at a given location “x” is given by:

$$PM(x) = PPM(x) + \min\{NO_x(x), NH_3(x)\}_{mole} \times NH_4^+NO_3^- \quad (4)$$

970



971 Figure A1: Schematic representation of the theoretical example used to compare the three SA approaches. The city source (in
 972 red) emits NO_x and PPM. The background (in blue, including other cities as well as rural sources) is composed of NO_x, PPM and
 973 NH₃ in different relative proportions (indicated by the arrow). The “cc” and “bg” symbols represent the city centre receptor and
 974 the background location used for the increment approach, respectively.
 975

976 Based on the formulations provided in Table 1 and equation (4), the expressions to calculate the
 977 city and background components for the theoretical example presented above are detailed in
 978 Table A1. While these formulations are relatively straightforward for potential impacts and
 979 increments, it is more complex for the tagging method. The city tagging component is the sum of
 980 all PM species that are directly related to the city emissions. This includes PPM and NO₃ that are
 981 related to the PPM and NO_x city emissions, respectively. For the background component, it
 982 includes PPM, NO_x and also NH₄ that is related to the NH₃ emissions. Tagging allows following
 983 the NO_x and NH₃ emitted compounds through their chemical processes and transformations until
 984 they create NO₃ and NH₄, respectively that can be attributed to their respective sources. As NO_x
 985 is emitted by both sources, the total NO₃ must be fractioned and attributed to each single source.

986 In our example, the NO₃ fraction attributed to the city depends on the ratio of the available NO_x
 987 precursor at the location of interest ($\beta = \frac{NO_{x,city}(cc)}{NO_{x}(cc)}$). A similar process is used to calculate the
 988 background component.

989 This example is used to compare the increment (INC), tagging (TAG) and potential impact (PI)
 990 SA approaches.

991
 992
 993

Potential Impact	
City	$PM_{city}^{PI\alpha}(cc) = \frac{PM(cc) - PM_{city}^{\alpha}(cc)}{\alpha}$
Background	$PM_{bg}^{PI\alpha}(cc) = \frac{PM(cc) - PM_{bg}^{\alpha}(cc)}{\alpha}$
Increment	
City	$PM_{city}^{INC}(cc) = PM(cc) - PM(bg)$
Background	$PM_{bg}^{INC}(cc) = PM(bg)$
Tagging	
City	$PM_{city}^{TAG}(cc) = \sum_E^{city} PM_E(cc) = PPM_{E(PPM)_{city}}(cc) + \beta NO_3^-_{E(NO_2)_{city}}(cc)$
Background	$PM_{bg}^{TAG}(cc) = \sum_E^{bg} PM_E(cc) = PPM_{E(PPM)_{bg}}(cc) + (1 - \beta) NO_3^-_{E(NO_2)_{bg}}(cc) + NH_4^+_{E(NH_3)_{bg}}(cc)$

994 Table A1: Formulations for the potential impacts, increments and tagging approach for the example presented in Figure A1. The
 995 indicator for all methods and components is the total particulate matter mass (PM). The SA method is indicated as superscript
 996 (PI α , INC or TAG) whereas the source (city or bg) is in subscript. The receptor is the city center (cc) while the rural location
 997 selected for the increment approach is denoted by "bg". For the tagging, the source subscript is also expressed directly as
 998 emissions (E) distinguishing each compound (within brackets).

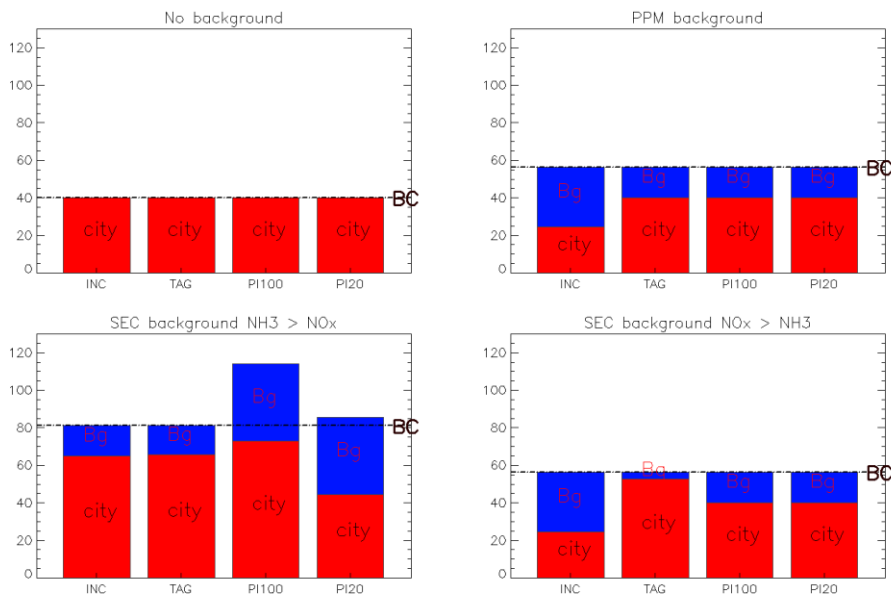
999 Figure -A2 shows the city and background contributions obtained with the three SA methods,
 1000 differentiating two options for the PI one: 100% (PI100) and 20% reduction of the sources
 1001 (PI20). The figure also distinguishes four situations characterized by different background
 1002 compositions.

- 1003
- 1004 1. **No background:** When no background is present (top left), the city NO_x emissions do not
 1005 form PM, only PPM emissions do. In such cases, all methods deliver the same response.
 1006
- 1007 2. **PPM background:** When the background is composed of PPM only (top right), no
 1008 secondary species are formed. All methods agree with the exception of the increment
 1009 approach. This is due to the non-fulfilment of one of its underlying assumptions, i.e. the
 1010 lack of spatial homogeneity of the background which affects differently the rural and city
 1011 locations (indicated by "cc" and "bg" in [Figure Figure A2](#), respectively).
 1012

Formatted: Font: (Default) Times New Roman, 12 pt

- 1013 3. SEC background with $\text{NH}_3 > \text{NO}_x$: When secondary background precursors (NO_x and
 1014 NH_3) reach the city (bottom row), SA methods deliver different results because they
 1015 manage differently non-linear processes. When NH_3 is more abundant than NO_x (bottom
 1016 left), the PII00 method does not preserve additivity (discussed in the “concepts” section),
 1017 i.e. the sum of the two components exceeds the total PM concentration. As seen from the
 1018 results and also from Table Table-A1, this is not the case for the increment and tagging
 1019 approaches that are constructed to be additive.
 1020
 1021 4. SEC background with $\text{NH}_3 < \text{NO}_x$: When NH_3 is less abundant than NO_x (bottom right),
 1022 differences remain important between the tagging, potential impacts and increment
 1023 approaches but additivity is preserved for both PII00 and PII0 that provide identical
 1024 responses.

Formatted: Font: (Default) Times New Roman, 12 pt, English (United States)



1025
 1026
 1027
 1028
 1029
 Figure A2: Comparison of the city (red) and background (blue) components for 4 approaches applied on the theoretical examples described in Figure A1. Results are expressed for different types of background: (top left) no background; (top right) background limited to PPM; (bottom left) background limited to secondary but with $\text{NH}_3 > \text{NO}_x$ and (bottom right) background limited to secondary but with $\text{NH}_3 < \text{NO}_x$.